JOURNAL OF CATALYSIS 151, 216–225 (1995)

On the Kinetics of CO Methanation on Nickel Surfaces

I. Alstrup

Haldor Topsøe Research Laboratories, Nymøllevej 55, DK-2800 Lyngby, Denmark

Received June 3, 1994; revised August 22, 1994

A microkinetic model for CO methanation on nickel based on CO dissociation and stepwise hydrogenation of surface carbon is presented. Very good agreement with the methanation rates measured on Ni(100) by Goodman *et al.* (*J. Catal.* 63, 226 (1980)) and on nickel foils by Polizzotti and Schwarz (*J. Catal.* 77, 1 (1982)) is obtained by assuming that the rate-controlling step is hydrogenation of surface methylidyne and by treating the coverage of reactive carbon, θ_C, as a parameter. For not too low H_2:CO ratios it seems to be a good approximation to keep θ_C constant. The validity of this approximation may be related to the observations that only a small part of the surface carbon is reactive and that the rate depends on previous treatments of the nickel surface supposed to create special sites. It is shown that previously published macrokinetic models, which can be tested, do not give rates in agreement with the single crystal and foil results. Analysis of the present model shows that the overall activation energy, E_a, of the reaction is mainly determined by the chemisorption energy of CO in the temperature range where E_a is almost constant. The order of the H_2 dependence derived from the kinetic model is close to 1 in the entire range of reaction conditions considered, while the order of the CO dependence is -1 at low temperatures increasing at the highest temperatures to between -0.12 and -0.06 depending on the total pressure.

1. INTRODUCTION

The methanation reaction has been studied intensively ever since its discovery by Sabatier and Senderens (1) at the turn of the century. Even in the past decade when the interest in the large scale application of the process for hydrocarbon synthesis from coal gasification has faded and the main industrial application has been the removal of trace amounts of CO from H_2-rich feed gases, numerous studies of the methanation reaction have appeared. Many of these studies have been concerned with the kinetics of the process and several models have been suggested. Until the middle of the 1970s it was widely believed that the methanation process proceeds through a CH_xO intermediate (2). However, IR studies at reaction conditions failed to show the presence of such an intermediate. Moreover, a number of studies showed that CO dissociates under methanation conditions and that the rate of hydrogenation of the surface carbon is close to the methanation rate (3, 4). Since then a number of studies of the steady-state methanation kinetics on supported nickel catalysts have been reported. Very recently, Yadov and Rinker (5) presented a phenomenological model based on a proposed Langmuir–Hinshelwood (LH) mechanism. They claimed that the model described well steady-state methanation rates measured at 503, 513, and 523 K, although a scatter plot showed large differences between measured and calculated rates. The model contains three adjustable parameters for each temperature. Yadav and Rinker (5) also gave a brief overview of the steady-state kinetic models proposed previously by Ho and Harriott (6), Dalmon and Martin (7), van Meerten *et al.* (8), Klose and Baerns (9), Hayes *et al.* (10), and Coenen *et al.* (11). Four of the models are of the LH type based on different assumptions about the mechanism. The most complicated model is the one proposed by Coenen *et al.* (11), which contains for each tempeature eight adjustable parameters. Dalmon and Martin (7) and Hayes *et al.* (10) found that none of the LH models tested could account for their results, and the latter authors fitted a power law to their data. Also, a number of transient kinetic studies of the methanation reaction have appeared. Happel *et al.* (12) and Biloen *et al.* (13) used isotopic switching technique. The former authors concluded that the rate-controlling steps involve hydrogenolysis of chemisorbed CH_x ($x = 0 - 3$) rather than only the dissociation of CO or the formation of the above-mentioned "enolic" intermediate. Biloen *et al.* (13) concluded that of the large carbidic overlayer (corresponding to several monolayers) which develops during steady-state reaction, only a small part (of the order of 0.1 of a monolayer) participates directly in the reaction.

In pioneering studies Goodman and co-workers investigated the methanation reaction on nickel single crystal surfaces (14, 15). Surface analysis using Auger electron spectroscopy under ultrahigh vacuum conditions was combined with rate measurements at elevated temperatures and pressures. Rates measured for Ni(100) and Ni(111) surfaces were very similar. The effective activation energy and the turnover numbers obtained for the single crystal surfaces were also essentially the same as

0021-9517/95 $6.00

the values reported previously for supported nickel catalysts. These results showed that the process is structure insensitive, which may appear surprising considering that the difficult dissociation of CO is structure sensitive (16). Because of the absence of transport restrictions in the single crystal studies the rates could be measured over a much larger range than possible for supported catalysts. Recently new studies of the methanation reaction on nickel single crystal surfaces by Bonzel and co-workers (17, 18) have demonstrated that the rate depends quite sensitively on the previous history of the sample. The rate could be increased by up to a factor of four during the experiment by a series of brief low-energy inert-gas ion bombardments and yet significant changes of the surface could not be detected. Berkó and Bonzel (18) suggested that structural changes which escape detection with LEED, but which can be correlated with a small high-temperature shoulder on the CO–TPD profile, were responsible for the increased reactivity.

The demonstration of the relevance of surface science studies for the understanding of catalytic processes on industrial catalysts provided by the above-mentioned studies of Goodman and co-workers has encouraged researchers to try bridging the gap between surface science studies and industrial catalysis by constructing microkinetic models for catalytic reactions. Ideally a microkinetic model is based on information from surface science studies identifying the important elementary steps and determining the rate constants and the energies necessary for the calculation of the equilibrium constants of the steps. Until now only a few such models based almost entirely on surface science studies have been reported. A pioneering example of microkinetic modelling was the work by Stoltze and Nørskov (19) on the ammonia synthesis reaction, based largely on measurements on single crystal iron surfaces in the Ertl group (20). In this case remarkable agreement was obtained with rate measurements for industrial catalysts over a large range of conditions. Crucial for success in this case was a correct description of the dissociative chemisorption of N_2. The accurate description of the subsequent steps, the parameters of which have not been directly measured, was fortunately less important. Also in most other cases the information from surface science experiments has necessarily been incomplete so that it must be supplemented by less directly determined values. Alstrup and Tavares (21) constructed a microkinetic model for carbon formation on nickel catalysts exposed to $CH_4 + H_2$ gas mixtures. The dissociative chemisorption of CH_4 on single crystal nickel surfaces has previously been thoroughly studied and the surface intermediates formed in the subsequent dehydrogenation steps have been identified and their vibrational frequencies measured. However, measurements of the binding energies of the intermediates are lacking. Recently Siegbahn and Panas (22) have developed an *ab initio* method for the calculation of the chemisorption bond energies for atoms and small molecules on metals which was shown to give accurate values in the cases where comparison with experimental values could be made. They used the method to calculate the bond energies of the CH_x, $x = 0 \cdots 3$, species on nickel surfaces (22). Alstrup and Tavares (21) used this information to construct the above-mentioned microkinetic model, which by adjustment of two rate constants gave excellent agreement with measured rates.

It is obvious to try to construct a similar microkinetic model for the methanation reaction on nickel surfaces. The chemisorption of the reactants in the methanation reaction, CO and H_2, on nickel single crystal surfaces is probably the most extensively studied chemisorption system. A large amount of information important for the construction of such a microkinetic model is thus readily available. However, while, as mentioned above, many empirical kinetic models have been suggested to account for rates measured on supported nickel catalysts, no attempts to construct a microkinetic model have been reported until now. In the present paper the obstacles preventing the construction of a complete microkinetic model based entirely on surface science or theoretical results for the steady-state methanation reaction on nickel are discussed and a model is provided by adding a very simple assumption to the available information. In the next section a set of probable elementary steps, which can be deduced from experiments, is presented. However, rates cannot be calculated on the basis of this set only, because one rate constant is not known and the coverage of reactive carbon cannot be derived. The missing information is dealt with in Section 3 and rates are calculated and compared with the published methanation results obtained by Goodman *et al.* (14) on Ni(100) and by Polizzotti and Schwarz (23) on nickel foil.

2. ELEMENTS OF A KINETIC MODEL

In the methanation experiments of Kelley *et al.* (24). CO_2 was produced at a level of about 2% of the CH_4. Consequently steps involving CO_2 need not be taken into account in constructing a semiquantitative kinetic model. This leads us to suggest that a mechanism based on the following elementary steps should form a good starting point for constructing a microkinetic model:

$$H_2 + 2* \rightleftarrows 2H* \quad [1]$$

$$CO + * \rightleftarrows CO* \quad [2]$$

$$CO* + * \rightleftarrows C* + O* \quad [3]$$

$$C* + H* \rightleftarrows CH* + * \quad [4]$$

$$CH* + H* \rightleftarrows CH_2* + * \quad [5]$$

$$CH_2* + H* \rightleftarrows CH_3* + * \quad [6]$$

$$CH_3* + H* \rightarrow CH_4 + 2* \quad [7]$$

$$O* + H* \rightarrow OH* + * \quad [8]$$

$$OH* + H* \rightarrow H_2O + 2*. \quad [9]$$

The symbols used have the usual meaning; i.e., the asterisk (*) signifies an empty site and chemical formulae with an asterisk at the end refer to an adsorbed species, i.e., $CO*$ signifies an adsorbed CO molecule. On the basis of the known sticking probabilities of CO and H_2 it can be calculated that the rates of chemisorption of CO and H_2 under the conditions of the experiments of Goodman *et al.* (14) are far higher than the overall methanation reaction rates. It is clearly a good approximation to regard steps [1] and [2] as quasi-equilibrium steps and to use the equilibrium constants for the calculation of the $CO*$ and $H*$ coverages. As the hydrogenation of surface oxygen and the desorption of H_2O are rapid (25) it is not necessary to take these species into account and step [3] can be treated as an irreversible step. Step [3] may not be a simple dissociation step as indicated, but the formation of carbon surface atoms from CO may be strongly enhanced by the presence of other surface species. It is assumed that the methane partial pressure is negligible so that step [7], the associative desorption of methane, can to a good approximation be treated as an irreversible step. This assumption is discussed below in Section 4.

If one of the reversible steps [4]–[6] or step [7] is a rate-controlling step (rcs) then using the steady-state condition the expression

$$\text{rate} = \frac{a_1 P_{H_2}^2 \theta_C \theta*}{1 + a_2 P_{H_2}^{n/2}} \quad [10]$$

is obtained, where

$$a_1 = k_7 K_4 K_5 K_6 K_1^2 \quad [11]$$

and if step [4] is rcs then $n = 3$ and

$$a_2 = \frac{k_7}{k_4} K_4 K_5 K_6 K_1^{3/2}; \quad [12]$$

if step [5] is rcs then $n = 2$ and

$$a_2 = \frac{k_7}{k_5} K_5 K_6 K_1; \quad [13]$$

if step [6] is rcs then $n = 1$ and

$$a_2 = \frac{k_7}{k_6} K_6 K_1^{1/2}; \quad [14]$$

if step [7] is rcs then $n = 0$ and

$$a_2 = 0. \quad [15]$$

The equilibrium constants of the steps (1) to (7), K_i, $i = 1 \cdots 7$, can be calculated from the partition functions Z_x, where x is the formula for a molecule or a chemisorbed species:

$$K_1 = \frac{Z_{H*}^2}{Z_{H_2}} \quad [16]$$

$$K_2 = \frac{Z_{CO*}}{Z_{CO}} \quad [17]$$

$$K_3 = \frac{Z_{C*} Z_{O*}}{Z_{CO*}} \quad [18]$$

$$K_4 = \frac{Z_{CH*}}{Z_{C*} Z_{H*}} \quad [19]$$

$$K_5 = \frac{Z_{CH_2*}}{Z_{CH*} Z_{H*}} \quad [20]$$

$$K_6 = \frac{Z_{CH_3*}}{Z_{CH_2*} Z_{H*}} \quad [21]$$

$$K_7 = \frac{Z_{CH_4}}{Z_{CH_3*} Z_{H*}}. \quad [22]$$

The partition functions can to a very good approximation be written as products of the contributions from all the degrees of freedom. The vibrational energies and chemisorption bond energies used in the calculations of the partition functions used to calculate K_1 and K_4–K_7 are presented and discussed in Ref. (21) and similarly the values needed for calculating Z_{CO} and Z_{CO*} can be found in Ref. (26). The vibrational energies are known from experiments with the exception of the frustrated translations of the chemisorbed species parallel to the surface, which is only known for CO on Ni(100) (27). Experimental values for the chemisorption bond energies are known for $H*$ and $CO*$. For the CH_x, $x = 0 \cdots 3$, species the bond energy values calculated by Siegbahn and Panas (22) are used. k_7 may be calculated from the dissociative sticking probability of CH_4 and K_7 by assuming detailed balance to hold. To be able to calculate the methanation rate using expression (10) values for the rate constant of the rate-controlling step and for the coverage θ_C of active carbon are needed. It is assumed that all the coverages of the

active sites are negligible with the exception of the coverage of active carbon atoms, of hydrogen atoms, and of CO molecules, which are all competing for the same sites, i.e.,

$$\theta* = (1 - \theta_C)/[1 + (K_1 P_{H_2})^{1/2} + K_2 P_{CO}]. \quad [23]$$

3. CALCULATED RATES COMPARED WITH EXPERIMENTAL SINGLE CRYSTAL AND FOIL RESULTS

Kelley and Semancik (28) deduced from a large number of combined rate and Auger electron spectroscopy measurements at 625 K that a universal relationship exists, at least at this temperature, between the rate of methanation and the carbon coverage corresponding to a coverage of about 0.05 monolayers (ML) at the highest rates and about 0.25 ML at the lowest ones (28). However, from the results of the above-mentioned transient studies, including the isotope switching experiments of Biloen *et al.* (13), it is expected that only a small part of the carbon determined by the Auger measurements is active in the methanation reaction. Surprisingly, it is found that excellent agreement can be obtained between the model and the experimental points of the Arrhenius plot of Goodman *et al.* (14), as shown in Fig. 1, by varying k_5 and k_7 and keeping the surface concentration of active carbon, θ_C, constant, independent of temperature and partial pressures. The experimental data were obtained for a large temperature range (450–800 K) and three total pressures, 1, 10, and 120 Torr (1 Torr = 133 Pa), but with a fixed H_2 : CO ratio equal to 4 : 1. In the calculations of the model rates it is assumed that step [5] is rate controlling. Good agreement is not obtained if it is assumed that step [4] or step [6] is rate controlling or if it is assumed that all the steps [4]–[6] are close to equilibrium.

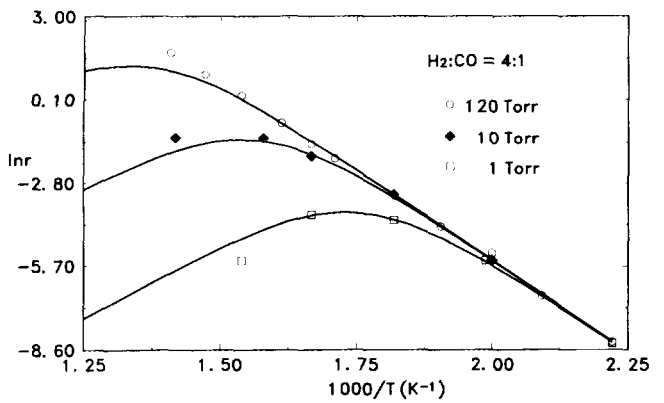

FIG. 1. Arrhenius plot of CO methanation rates on Ni(100), H_2: CO = 4 : 1. Experimental points from Ref. (14). P_{total} = 1 Torr (□), 10 Torr (◆), and 120 Torr (○). Curves are calculated using the microkinetic model.

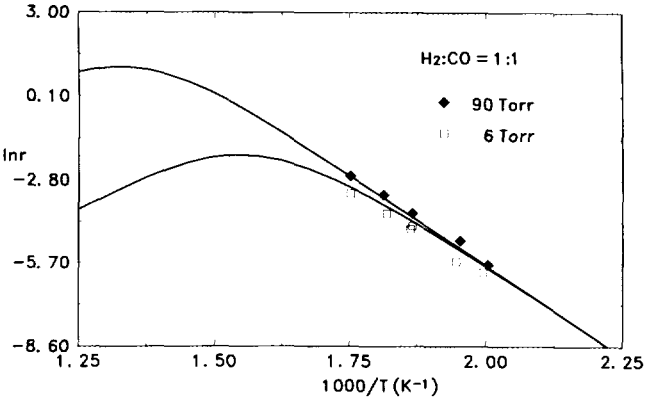

FIG. 2. Arrhenius plot of CO methanation rates on Ni foil, H_2: CO = 1 : 1. Experimental points from Ref. (23). P_{total} = 6 Torr (□) and 90 Torr (◆). Curves are calculated using the microkinetic model.

Goodman and co-workers have unfortunately not published results which allow testing the rate expression for other H_2:CO ratios. However, Polizzotti and Schwarz (23) have made methanation rate measurements on polycrystalline nickel foils for several H_2 : CO ratios, 1 : 1, 2 : 1, 3 : 1, 15 : 1, and 30:1, and total pressures from 5 to 200 Torr and in the temperature range 423–673 K. The model rates also agree with these results using the same constant θ_C if we take into account that the reactivity of the surface may depend quite strongly on the history of the sample as shown by the results of Bonzel and coworkers (17, 18). The variability of the reactivity is also seen in the results of Goodman and co-workers; e.g., from the Arrhenius plot in Ref. (14) it appears that at 625 K and 10 Torr the turnover number on Ni(100) is about 0.25, while from the plot of rates versus carbon coverage in Ref. (28) it appears that the turnover number is about 0.07 in the same conditions. This may also explain why some of the results of Polizzotti and Schwarz (23) show a strange pressure dependence: The rates corresponding to a total pressure of 6 and 90 Torr for H_2 : CO = 15 : 1 are close together, while the rates corresponding to 10 Torr are significantly below the rates measured at 6 and 90 Torr. In comparing the model with the results of Polizzotti and Schwarz (23), as shown in Figs. 2–6, the model rates have been multiplied by a factor between 0.4 and 3. The scaling factors used are shown in Table 1. In most cases the scaling factor depends only on the H_2:CO ratio with the above-mentioned case, H_2 : CO = 15 : 1, as a clear exception. The monotonic increase in the scaling factor when the H_2 : CO ratio is decreased from 3 : 1 to 1 : 1 may indicate that the concentration of reactive carbon increases when the ratio is decreased in this range. This tendency is not seen at the higher ratios, e.g., at H_2 : CO = 30 : 1, where excellent agreement is obtained using a scaling factor equal to one. It is noteworthy that the model rates

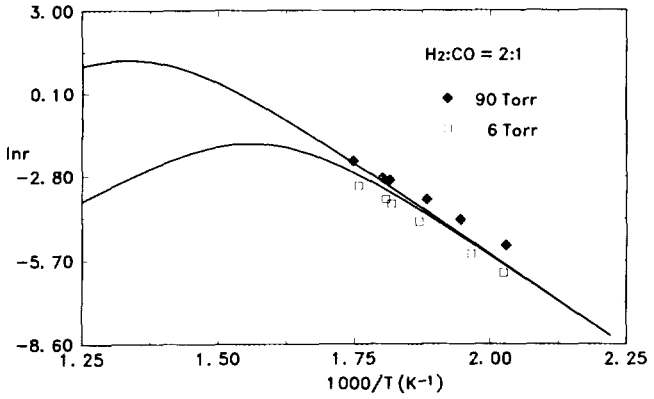

FIG. 3. Arrhenius plot of CO methanation rates on Ni foil, H_2: CO = 2 : 1. Experimental points from Ref. (23). P_{total} = 6 Torr (□) and 90 Torr (◆). Curves are calculated using the microkinetic model.

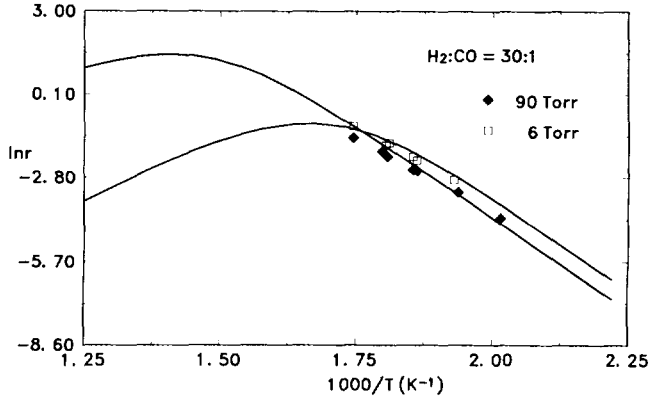

FIG. 6. Arrhenius plot of CO methanation rates on Ni foil, H_2: CO = 30 : 1. Experimental points from Ref. (23). P_{total} = 6 Torr (□) and 90 Torr (◆). Curves are calculated using the microkinetic model.

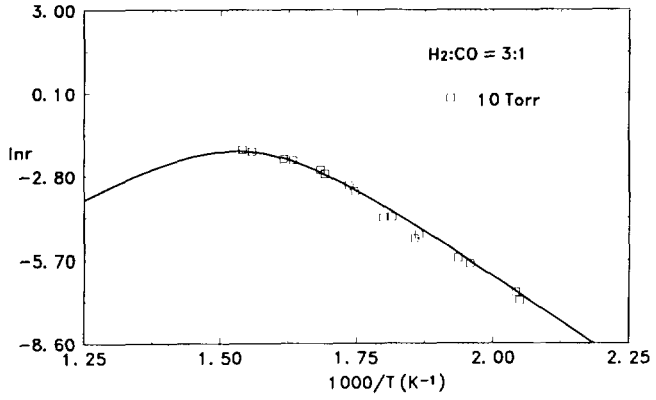

FIG. 4. Arrhenius plot of CO methanation rates on Ni foil, H_2: CO = 3 : 1. Experimental points from Ref. (23). P_{total} = 10 Torr (□). Curves are calculated using the microkinetic model.

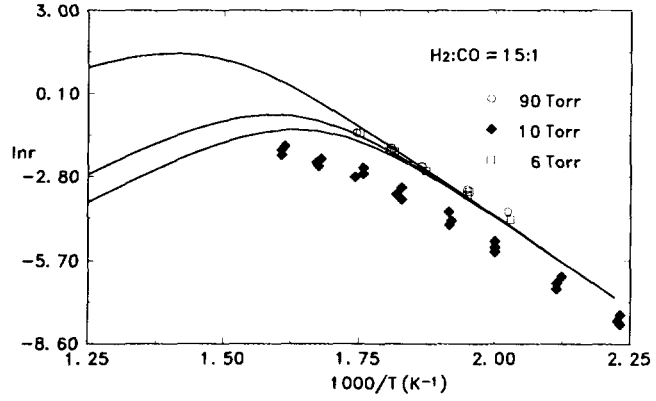

FIG. 5. Arrhenius plot of CO methanation rates on Ni foil, H_2: CO = 15 : 1. Experimental points from Ref. (23). P_{total} = 6 Torr (□) and 10 Torr (◆), and 90 Torr (○). Curves are calculated using the microkinetic model.

show at this high ratio and low temperature the same reversal of the pressure dependence as the experimental rates.

4. DISCUSSION

The observations mentioned in the Introduction, that a "pool" of carbon, which does not participate directly in the process, is present on/in the surface during the reaction and that the rate depends on the previous history of the surface, indicate that it might be difficult to establish a steady-state microkinetic model for methanation on nickel surfaces. The dependence on the history of the sample may explain the lack of accurate reproducibility indicated by some of the results of Goodman and coworkers, as mentioned above. The considerable number

TABLE 1

Scaling of Model Rates[a]

H_2 : CO	P_{total} (Torr)	Scaling factor
1 : 1	6 and 90	3.0
2 : 1	6 and 90	2.0
3 : 1	10	0.6
4 : 1	1, 10, and 120	1.0
15 : 1	6 and 90	1.0
15 : 1	10	0.4
30 : 1	6 and 90	1.0

[a] The model rates are multiplied by the scaling factor to obtain close agreement with experimental rates. The experimental rates are from Ref. (23) with the exception of the results for H_2 : CO = 4 : 1, which are from Ref. (14).

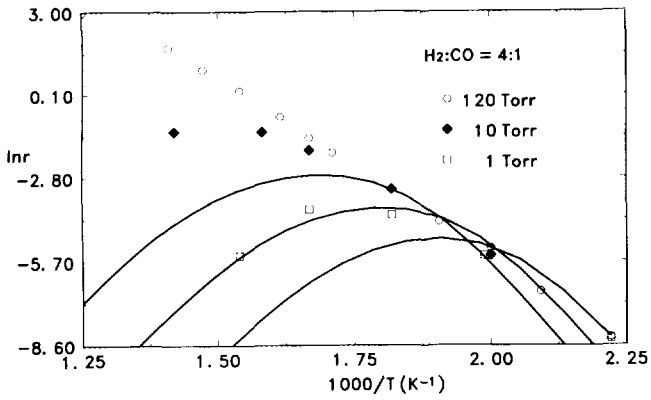

FIG. 7. Comparison between experimental CO methanation rates on Ni (100) from Ref. (14) (see Fig. 1) and rates calculated using the model from Ref. (5).

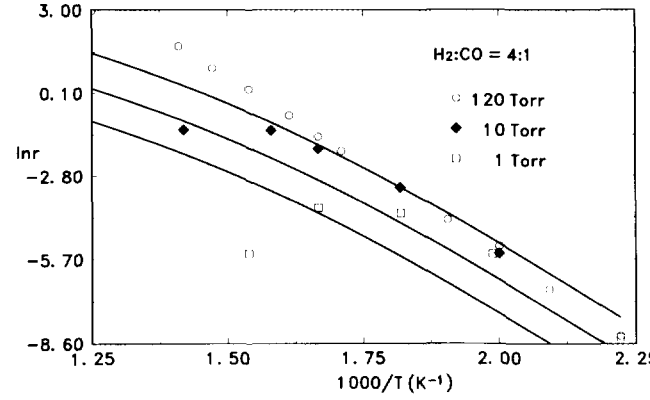

FIG. 9. Comparison between experimental CO methanation rates on Ni (100) from Ref. (14) (see Fig. 1) and rates calculated using the model from Ref. (11).

of different kinetic models suggested for this process may also be related to these facts. The comparisons in Figs. 7–9 of methanation rates using the models for which parameter values have been published, i.e., the models suggested by Yadav and Rinker (5), by van Meerten *et al.* (8), and by Klose and Baerns (9), with the single crystal results of Goodman *et al.* (14) show that none of these models can account for the single crystal results. The model rates have been scaled so that agreement has been obtained with the experimental rate at 550 K and P_{total} = 120 Torr.

In contrast to the above, the present model gives an accurate account of the single crystal and the nickel foil results. The model is based on the set of elementary steps [1]–[7]. Because the concentration of reactive carbon is assumed to be a constant independent of temperature and pressure within the broad ranges considered, it is unimportant how the reactive surface carbon atoms are produced from CO and how step [3] is written. It was suggested above that step 7 can be treated as an irreversible step. This assumption may need justification. Goodman *et al.* (14) and Polizzotti and Schwarz (23) used a batch reactor but did not report the CH_4 pressure which was built up in the reactor during an experiment. However, Goodman *et al.* (14) stated that the amount of CH_4 produced during an experiment was below 1%. An upper limit of the rate of readsorption of CH_4, r_a, can therefore be calculated on the basis of the rates of the dissociative chemisorption of CH_4 on Ni(100) measured by Chorkendorff *et al.* (29). The results of such a calculation for the conditions of the experimental results in Fig. 1 are shown in Table 2. The clean surface sticking coefficient is taken from Ref. (29), while expression [23] is used to calculate $\theta*$. It is seen that r_a is about four orders of magnitude lower than the methanation rate at the lowest temperature, while at the highest temperature it is only about an order of magnitude lower. The model may therefore be expected to be less accurate at the highest temperatures. However, the calculation is based on the simple assumption that for the chemisorption of CH_4 on Ni(100) only one free site is required, while it has been shown in Ref. (29) that a free site plus free nearest neighbor sites are required. It is therefore conceivable that the adsorption of CH_4 is negligible also at the highest temperatures. Polizzotti and Schwarz (23) have conducted their experiments in the same way as Goodman *et al.* (14) and measured rates in the same range, so it is to be expected that the above justification for neglecting readsorption of methane can be applied to all the results considered.

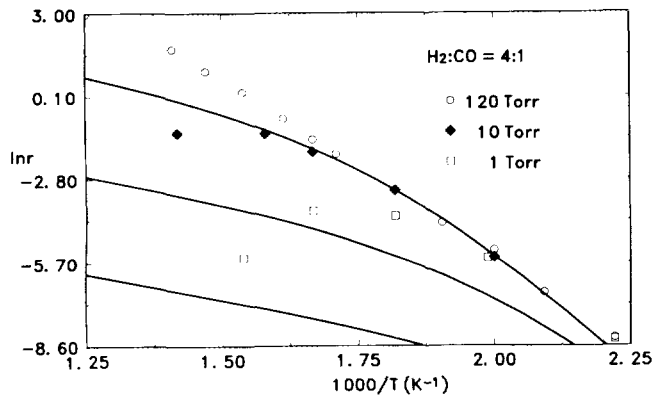

FIG. 8. Comparison between experimental CO methanation rates on Ni (100) from Ref. (14) (see Fig. 1) and rates calculated using the model from Ref. (9).

As mentioned above, the model is based on the simple but apparently arbitrary assumption that the surface concentration of the reactive carbon atoms is independent of temperature and partial pressures within a broad range. This assumption is justified primarily by the excellent

TABLE 2
Rate of CH_4 Adsorption, r_a, When $P_{CH_4} = 0.01 \times P_{total}$

T(K)	r_a (ML s^{-1})	Model rate (ML s^{-1})
	P_{total} = 120 Torr	
450	1.7×10^{-8}	2.4×10^{-4}
487	5.1×10^{-7}	2.1×10^{-3}
597	1.0×10^{-3}	2.4×10^{-1}
708	1.1×10^{-1}	3.0
	P_{total} = 10 Torr	
450	1.7×10^{-8}	2.4×10^{-4}
487	5.1×10^{-7}	2.1×10^{-3}
597	8.8×10^{-4}	1.6×10^{-1}
708	2.1×10^{-2}	1.8×10^{-1}
	P_{total} = 1 Torr	
450	1.7×10^{-8}	2.4×10^{-4}
487	5.1×10^{-7}	1.8×10^{-3}
597	3.5×10^{-4}	2.0×10^{-2}
708	1.1×10^{-3}	8.1×10^{-1}

agreement between model and experimental results. Such an agreement could not be obtained by assuming that the coverage of reactive carbon is provided by a steady-state balance between carbon formation and carbon removal by steps [1]–[9]. A further justification of the model is that some of the crucial parameters used to obtain the best agreement with the results of Goodman *et al.* show good agreement with previously established values. The agreement has been obtained by using Arrhenius expressions for the rate constants k_5 and k_7 with pre-exponential factors and activation energies as shown in Table 3. It should be noted that the preexponential factors shown are very uncertain because they depend on the assumed coverage of reactive carbon, θ_C. Also, a weak temperature dependence influencing the activation energies cannot be excluded. In the model rate calculations it was assumed that θ_C = 0.05 ML, corresponding to the lowest carbon coverage measured by Goodman and co-workers and consistent with the surface coverage of reactive carbon estimated by Biloen *et al.* (13). The chemisorption bond energies used for hydrogen atoms and CO molecules in the model are 245 kJ/mol and 120 kJ/mol, respectively. The hydrogen value is the one used previously in modelling the kinetics of the decomposition of CH_4 on a nickel catalyst (21). It was shown recently that the value is in good agreement with the carbon and hydrogen coverage dependences of hydrogen temperature-programmed desorption (30).

TABLE 3
Rate Constants $k_i = k_{0,i} \exp(-E_i/RT)^a$

$k_{0,5}$ ($ML^{-1}s^{-1}$)	E_5 (kJ/mol)	$k_{0,7}$ ($ML^{-1}s^{-1}$)	E_7 (kJ/mol)
7.26×10^7	26.8	5.80×10^{10}	30.8

[a] Best fit for θ_C = 0.05 ML.

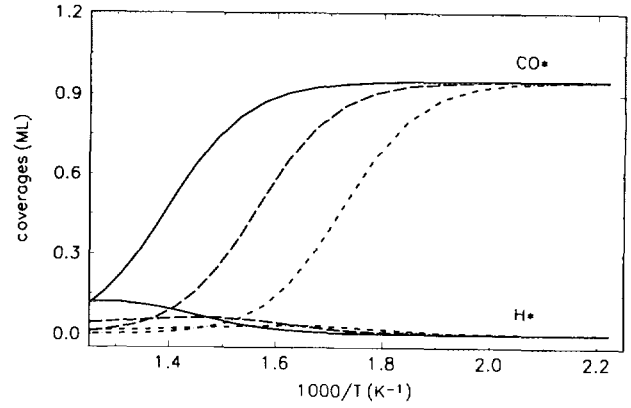

FIG. 10. Microkinetic model coverages during CO methanation on nickel as functions of temperature and pressure. P_{total} = 120 Torr (—), 10 Torr (---), and 1 Torr (-·-).

The activation energy, E_7, of k_7 can be determined from the activation energy, E_{ch}, of CH_4 chemisorption and the van't Hoff enthalpy, ΔH_7, of the equilibrium constant K_7 provided detailed balance holds. E_{ch} = 52 kJ/mol (29) and ΔH_7 is in the range 20.0–15.3 kJ/mol in the temperature range 450–650 K. This means that E_7 should be in the range 29.8–34.5 kJ/mol if the $1/\sqrt{T}$ dependence of the adsorption flux is also taken into account. This range is seen to be in good agreement with the E_7 value in Table 3. The results of Bonzel and co-workers (18) that the methanation rates were enhanced by up to four times by a number of mild sputtering treatments are also consistent with the assumption of a constant surface concentration of reactive carbon provided the formation of reactive carbon depends on special sites which can be created by sputtering and which can survive under reaction conditions. The methanation reactivity of a nickel surface then depends on the small number of such special sites created in the surface preparation process and surviving the transient reaction period before steady state is achieved. It may be possible to elucidate the existence and nature of such sites by means of scanning tunnelling microscopy.

The CO* and H* coverages calculated are plotted vs $1000/T$ in Fig. 10. By comparison with Fig. 1 it is seen that the CO* coverage is high in the range where the logarithm of the rate, $\ln r$, is a linear function of T^{-1}, but decreases rapidly when $\ln r$ begins to bend down. More

TABLE 4

ΔH_i (kJ/mol) of the Equilibrium Constants $K_i = A_i \exp(-\Delta H_i/RT)$

T(K)	ΔH_1	ΔH_2	ΔH_4	ΔH_5	ΔH_6
450	−51.81	−118.8	12.27	5.38	−28.36
650	−48.69	−116.9	9.25	3.58	−30.79

detailed information as to which physical properties determine the temperature dependence of the rate is obtained by calculating the contributions to the effective activation energy, E_a, of the rate

$$E_a = -R\frac{1}{r}\frac{\partial r}{\partial(1/T)}, \qquad [24]$$

where R is the gas constant and the rate r is given by expressions [10] and [13]. Inserting in [24] gives

$$E_a = \Delta H_1 + \Delta H_4 - B + C + D, \qquad [25]$$

where ΔH_i is the van't Hoff enthalpy of the equilibrium constant K_i and

$$B = \frac{\Delta H_2 K_2 P_{CO} + 1/2\Delta H_1 K_1^{1/2} P_{H_2}^{1/2}}{1 + K_2 P_{CO} + K_1^{1/2} P_{H_2}^{1/2}} \qquad [26]$$

$$C = E_5 \frac{A}{1+A} \qquad [27]$$

$$A = \frac{k_7}{k_5} K_5 K_6 K_1 P_{H_2} \qquad [28]$$

$$D = (E_7 + \Delta H_5 + \Delta H_6 + \Delta H_1)\frac{1}{1+A}. \qquad [29]$$

The enthalpies ΔH_i at 450 and 650 K are shown in Table 4 and the values of A, B, C, D, and E_a are shown in Tables 5–7 at the same two temperatures for the total pressures 120, 10, and 1 Torr, respectively. It is seen that $A \gg 1$ at low temperatures, which means that C is almost equal to E_5 and D is small as seen in Tables 5–7. B is almost equal to ΔH_2 at low temperature and as the other contributions

TABLE 5

E_a(kJ/mol) at P_{H_2} = 96 Torr and P_{CO} = 24 Torr

T(K)	A	B	C	D	E_a
450	4143.72	−118.8	26.75	−0.01	105.9
650	11.87	−102.4	24.67	−3.51	84.1

TABLE 6

E_a (kJ/mol) at P_{H_2} = 8 Torr and P_{CO} = 2 Torr

T(K)	A	B	C	D	E_a
450	345.31	−118.5	26.67	−0.13	105.9
650	0.9892	−48.9	13.30	−22.70	0.1

to E_a are smaller and almost cancel out, E_a is approximately equal to ΔH_2. This means that the blocking of the surface due to chemisorption of CO controls the rate at low temperatures. A is small at 650 K and at low hydrogen pressure and B is also much smaller than ΔH_2 at 650 K because $K_2 P_{CO}$ is no longer much larger than 1 and the rate curves bend down.

The rate expression is not dependent on how the active carbon is formed. In the list of elementary steps it is suggested that carbon formation takes place by dissociation of CO*, step [3]. Carbon formation on nickel catalysts has been discussed by many authors and most recently by Tavares *et al.* (26). In the latter paper it was concluded that at very low CO pressures carbon formation takes place by the dissociation of CO* while at higher pressures disproportionation dominates, i.e., the dissociation of a CO* molecule is enhanced by the presence of a neighboring CO molecule, which extracts the oxygen atoms to form a CO_2 molecule. The kinetic results obtained by Astaldi *et al.* (31) in the temperature range 453–573 K and at CO pressures up to 2.3×10^{-6} Torr were best described by assuming that the rate-determining step is dissociation of CO, while, e.g., the results of Tavares *et al.* (26) in the temperature range 583–713 K and at CO pressures down to about 0.08 Torr were best described by assuming that disproportionation of CO is dominating. This means that the borderline CO coverage is about 0.01 ML and that CO-assisted disproportionation of CO dominates at low temperatures in the reaction conditions considered here. Astaldi *et al.* (31) determined the rate constant for CO dissociation at low pressure on Ni(100) to be $k_{dis} = 5.4 \times 10^9 \exp(-E_{dis}/RT)$, where E_{dis} = 97.9 kJ/mol. Dissociation rates calculated using k_{dis} are smaller than the methanation rates in Fig. 1 at temperatures below about 600 K. CO or hydrogen enhancement of the dissociation rate of CO is thus needed

TABLE 7

E_a (kJ/mol) at P_{H_2} = 0.8 Torr and P_{CO} = 0.2 Torr

T(K)	A	B	C	D	E_a
450	34.53	−116.5	25.99	−1.24	101.7
650	0.0989	−8.74	2.41	−41.09	−69.4

in this temperature range to explain the observed steady-state methanation rates.

In kinetic studies of the methanation process it is common practice to characterize the CO and H_2 dependences of the rate by stating orders with respect CO and H_2 (9). The orders α_{CO} and α_{H_2} are defined by the power-law expression

$$\text{rate} = f(T) \times P_{CO}^{\alpha_{CO}} P_{H_2}^{\alpha_{H_2}}. \quad [30]$$

Generally a positive value close to or equal to one has been found for α_{H_2}, while for α_{CO} negative as well as positive values have been mentioned, ranging between -1 and $+0.5$ (9). The exponents can be calculated by means of the formula

$$\alpha_i = P_i \frac{\partial \ln r}{\partial P_i}, \quad [31]$$

where i means either CO or H_2. For the present kinetic model the expressions

$$\alpha_{CO} = -\frac{K_2 P_{CO}}{1 + K^{1/2} P_{H_2}^{1/2} + K_2 P_{CO}} \quad [32]$$

and

$$\alpha_{H_2} = 2 - \frac{1/2 K_1^{1/2} P_{H_2}^{1/2}}{1 + K_1^{1/2} P_{H_2}^{1/2} + K_2 P_{CO}} - \frac{a_2 P_{H_2}}{1 + a_2 P_{H_2}} \quad [33]$$

are obtained.

For the range of conditions corresponding to the experimental results of Goodman *et al.* (14) in Fig. 1 α_{H_2} is essentially equal to 1 for all temperatures when the total pressure is 120 Torr. At the lower pressures α_{H_2} is slightly below one at the highest temperatures (3 and 6% below for P_{total} equal to 10 and 1 Torr, respectively). α_{CO} is shown as a function of temperature and total pressure in Fig. 11. It varies from -1 at low temperatures to between -0.12 and -0.06 at the highest temperatures depending on the pressure.

In constructing the model it was assumed that the carbon coverage entering the kinetic expression stays constant independent of the reaction conditions. Thus it is assumed that the "unreactive" carbon formed is not influencing the sites which are important for the methanation reaction. The model may be modified to take into account the possibility that unreactive carbon is blocking sites where hydrogen atoms or CO molecules, taking part in the reaction, could be adsorbed. This can be done simply by replacing the factor $(1 - \theta_C)$ in expression [23] by $(1 - \theta_{C,tot})$, where $\theta_{C,tot}$ is the sum of the surface

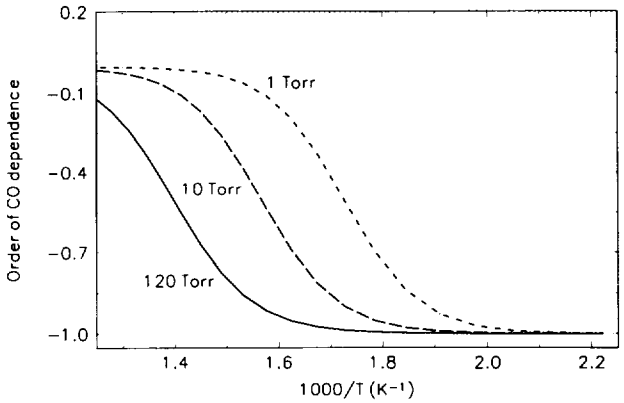

FIG. 11. Order of the CO dependence of the microkinetic model rates as functions of temperature and pressure. P_{total} = 120 Torr (—), 10 Torr (---), and 1 Torr (-·-).

concentrations of reactive and unreactive carbon. Important for the agreement of the model with the experimental results is that the product $\theta_C(1 - \theta_{C,tot})$ is approximately constant and in the range 0.03–0.13 independent of temperature and pressure. A small deviation from constancy is of course possible. If $\theta_{C,tot}$ is determined from the universal relationship between rate and carbon coverage deduced by Kelley and Semancik (28) a significant deviation from the experimental results is seen at the lowest temperature only. In this connection it is worth mentioning that a very recent high-resolution X-ray photoelectron spectroscopy and low-energy electron diffraction study by Zdansky *et al.* (32) may explain why a large part of the carbon atoms deposited on the nickel surface does not participate in the methanation reaction and why these carbon atoms are not blocking the surface. Zdansky *et al.* (32) concluded from the results that carbon atoms deposited on a Ni(100) surface migrate reversibly to subsurface positions when CO is adsorbed on the surface. The experiments were carried out at low CO pressures and low temperatures.

6. SUMMARY

It is shown that published macrokinetic models, which can be tested, do not give rates in agreement with the rates measured on nickel single crystals and foils. A microkinetic model is constructed based on the formation of reactive surface carbon by decomposition of CO and stepwise hydrogenation of surface carbon. The coverage by reactive carbon, θ_C, is assumed to be constant in the range of reaction conditions considered. Very good agreement is obtained with the single crystal and foil results by assuming that the hydrogenation of CH* is rate controlling. The validity of the assumption of a constant θ_C may be related to the fact that only a small part of the

surface carbon takes part in the reaction and that the steady-state reaction rates have been shown to depend on previous treatments of the nickel surface supposed to create special sites. Analysis of the model shows that the CO coverage is high and almost constant in the temperature range where the overall activation energy, E_a, of the reaction is constant. It also shows that in this range E_a is mainly determined by the chemisorption energy of CO. The order of the hydrogen dependence of the model rate is close to 1 under all conditions, while the order of the CO dependence is -1 at low temperatures (450 K) but approaches a small negative value at the highest temperatures (650–710 K).

ACKNOWLEDGMENT

The author gratefully acknowledges support by the Danish Research Councils through the Center for Surface Reactivity.

REFERENCES

1. Sabatier, P., and Senderens, J. B., *C. R. Acad. Sci., Paris* **134,** 514 (1902).
2. Mills, G. A., and Steffgen, F. W., *Catal. Rev.* **8,** 159 (1973).
3. Wentrcek, P. R., Wood, B. J., and H. Wise, *J. Catal.* **43,** 363 (1976).
4. Goodman, D. W., Kelley, R. D., Madey, T. E., and White, J. M., *J. Catal.***64,** 479 (1980).
5. Yadav, R., and Rinker, R. G., *Can. J. Chem. Eng.* **71,** 202 (1993).
6. Ho, S. V., and Harriott, P. *J. Catal.* **64,** 272 (1980).
7. Dalmon, J. A., and Martin, G. A., *J. Catal.* **84,** 45 (1983).
8. van Meerten, R. Z. C., Vollenbroek, J. G., de Croon, M. H. J. M., van Nisselrooy, P. F. M. T., and Coenen, J. W. E., *Appl. Catal.* **3,** 29 (1982).
9. Klose, J., and Baerns, M., *J. Catal.* **85,** 105 (1984).
10. Hayes, R. E., Thomas, W. J., and Hayes, K. E., *J. Catal.* **92,** 312 (1985).
11. Coenen, J. W. E., van Nisselrooy, P. F. M. T., de Croon, M. H. J. M., van Dooren, P. F. H. A., and van Meerten, R. Z. C., *Appl. Catal.* **25,** 1 (1986).
12. Happel, J., Cheh, H. Y., Otarod, M., Ozawa, S., Severdia, A. J., Yoshida, T., and Fthenakis, V., *J. Catal.* **73,** 314 (1982).
13. Biloen, P., Helle, J. N., van den Berg, F. G. A., and Sachtler, W. M. H., *J. Catal.* **81,** 450 (1983).
14. Goodman, D. W., Kelley, R. D., Madey, T. E., and Yates, J. T., *J. Catal.* **63,** 226 (1980).
15. Kelley, R. D., and Goodman, D. W., in "The Chemical Physics of Solid Surfaces and Heterogeneous Catalysis" (D. A. King and D. P. Woodruff, Eds.), Vol. 4, p. 427. Elsevier, Amsterdam, 1982.
16. Erley, W., and Wagner, H., *Surf. Sci.* **74,** 333 (1978).
17. Berkó, A., Coenen, F. P., and Bonzel, H. P., *Vacuum* **41,** 147 (1990).
18. Berkó, A., and Bonzel, H. P., *Surf. Sci.* **251/252,** 1112 (1991).
19. Stoltze, P., and Nørskov, J. K., *Phys. Rev. Lett.* **55,** 2502 (1985).
20. Grunze, M. in "The Chemical Physics of Solid Surfaces and Heterogeneous Catalysis" (D. A. King and D. P. Woodruff, Eds.), Vol. 4, p. 143. Elsevier, Amsterdam, 1982.
21. Alstrup, I., and Tavares, M. T., *J. Catal.* **135,** 147 (1992).
22. Siegbahn, P. E. M., and Panas, I., *Surf. Sci.* **240,** 37 (1990).
23. Polizzotti, R. S., and Schwarz, J. A., *J. Catal.* **77,** 1 (1982).
24. Kelley, R. D., Madey, T. E., Revesz, K., and Yates, J. T., *Appl. Surf. Sci.* **1,** 266 (1978).
25. Labohm, F., Gijzeman, O. L. J., and Geus, J. W., *Surf. Sci.* **135,** 409 (1983).
26. Tavares, M. T., Alstrup, I., Bernardo, C. A., and Rostrup-Nielsen, J. R., *J. Catal.* **147,** 525 (1994).
27. Berndt, R., Toennies, J. P., and Wöll, Ch., *J. Electron. Spectrosc.* **44,** 183 (1987).
28. Kelley, R. D., and Semancik, S., *J. Catal.* **84,** 248 (1983).
29. Chorkendorff, I., Alstrup, I., and Ullmann, S., *Surf. Sci.* **227,** 291 (1990).
30. Alstrup, I., Chorkendorff, I., and Ullmann, S., *Surf. Sci.* **293,** 133 (1993).
31. Astaldi, C., Santoni, A., Della Valle, F., and Rosei, R., *Surf. Sci.* **220,** 322 (1989).
32. Zdansky, E. O. F., Nilsson, A., and Mårtensson, N., *Surf. Sci. Lett.* **310,** 583 (1994).